Quasiperiodic synchronization for two delay-coupled semiconductor lasers

A. Hohl,[1] A. Gavrielides,[1] T. Erneux,[2] and V. Kovanis[1,3]
[1]*Nonlinear Optics Group, Air Force Research Laboratory, 3550 Aberdeen Avenue SE, Kirtland AFB, New Mexico 87117-5776*
[2]*Université Libre de Bruxelles, Optique Nonlinéaire Théorique Campus Plaine, Code Postal 231, 1050 Bruxelles, Belgium*
[3]*Department of Mathematics and Statistics, University of New Mexico, Albuquerque, New Mexico 87131*
(Received 20 August 1997; revised manuscript received 22 September 1998)

The dynamical behavior of two mutually coupled semiconductor lasers is studied experimentally, numerically, and analytically for weak coupling. The lasers have dissimilar relaxation oscillation frequencies and intensities, and their mutual coupling strength may be asymmetric. We find experimentally that the lasers preferentially entrain to the relaxation oscillation frequency of either one of the lasers. But quasiperiodic synchronization, where both relaxation oscillation frequencies appear, is possible. We show that there exist two distinct mechanisms leading to these regimes corresponding to either a bifurcation to a mixed-mode solution or a bifurcation induced by the delay of the mutually injected signal. However, only the second transition can be observed experimentally if the injection strength is continuously increased from zero.
[S1050-2947(99)00705-2]

PACS number(s): 42.65.Sf, 42.55.Px

I. INTRODUCTION

Coherent semiconductor laser arrays are a potential high-power coherent light source with applications in free-space communication and laser radar systems. The requirements to be met for these systems are challenging: high coherence, high power, narrow diffraction limited beam, and stable, single frequency operation. Since the first phase-locked semiconductor laser array was reported by Scifres *et al.* [1], a tremendous amount of research has been dedicated to studying the beam quality and spatial coherence properties of such devices [2] and less research has been dedicated to their temporal characteristics. Elliott *et al.* [3] have performed streak camera experiments on a semiconductor laser array consisting of ten coupled stripes. The authors observed that the intensity of the individual stripes exhibited strong and irregular spiking of 100–200 ps duration. Wang and Winful [4] used a time-dependent coupled mode theory to investigate the stability of such an evanescently coupled array. In this model the lasers are described by single mode rate equations and are coupled to their nearest neighbors. They found strong undamped relaxation oscillations in the individual array elements that evolved into irregular spiking behavior just as in the experiment. Both the theoretical and experimental results strongly suggest that the temporal behavior of coupled semiconductor laser arrays is very rich and complex. Yet, understanding the temporal behavior of an array of coupled semiconductor lasers is essential for building a stable device.

Systems of coupled lasers are also very interesting from the point of view of synchronization. A successful device of coupled lasers will require quality synchronization between lasers. Traditionally, synchronization describes frequency entrainment in a system of individual elements that have slightly different intrinsic frequencies but that lock to one common frequency when weakly coupled [5]. Synchronization in a set of coupled oscillators is typically modeled mathematically by considering units of identical oscillators with the same amplitude but slightly different frequencies that are symmetrically coupled [6]. Synchronization is found when the spread of the oscillating frequencies is not too large. In an array of coupled lasers, however, the individual lasers may exhibit intensity oscillations with quite different amplitudes and frequencies due to manufacturing constraints. Also the coupling between the lasers need not to be symmetric. The possible forms of synchronization between these different oscillators are much harder to predict theoretically and may depend on the particular laser system considered, such as solid state versus semiconductor lasers or evanescently coupled versus mutually coupled.

Synchronization of evanescently coupled identical semiconductor lasers has been demonstrated numerically in the chaotic regime by Winful and Rahman [8]. Experimentally, Roy and Thornburg [9] demonstrated that two coupled Nd:YAG lasers exhibit synchronized chaotic fluctuations. In both examples great care was taken that the elements were sufficiently identical to ensure good synchronization. But experimental observations by Thornburg *et al.* [10] on spatially coupled Nd:YAG lasers reveal amplitude and phase instabilities as the lasers are detuned in optical frequency for a given coupling strength. Moreover, numerical studies of the laser rate equations for this system show that more complex oscillatory patterns appear as soon as the difference between the individual laser pumping levels is changed [11]. This motivates bifurcation studies of the two coupled laser equations.

One form of synchronization, called localized synchronization, was recently analyzed by Kuske and Erneux [7] for a system of two coupled solid-state lasers. Localized synchronization appears when one or more oscillators in a coupled array exhibit large amplitude oscillations whereas the remaining oscillators exhibit small oscillations. In [7], two identical lasers are detuned by an optical frequency difference which nearly equals the relaxation oscillation frequency. Three coexisting solutions are found. Depending on the initial conditions there is one stable solution for which the oscillation amplitude of each laser is identical and there are two stable solutions for which the amplitude of oscillation is localized. These localized states become the dominant

 ©1999 The American Physical Society

attractors if the pump parameters of each individual laser are different.

In [12] we showed that localized synchronization between two mutually coupled semiconductor lasers was possible through a primary Hopf bifurcation mechanism. Depending on the values of the coupling parameters, one laser forces the other laser to oscillate at its relaxation oscillation frequency (i.e., at frequency f_1 or frequency f_2). However, a single mode synchronization is not the only possible form of interaction between lasers. Mixed mode forms of synchronization exhibiting the two individual laser relaxation oscillations frequencies are physically possible. As we shall demonstrate in this paper, these mixed-mode regimes may appear through a secondary bifurcation mechanism. By contrast to the localized states, the mixed states are quasiperiodic (with frequencies f_1 and f_2) and the two oscillation intensities are comparable in amplitude. Our analysis of the laser equations shows that they can be stable attractors but they may be harder to find experimentally. This competition between single mode and mixed-mode regimes is a key problem for all two coupled lasers systems. However, an important feature of our semiconductor laser problem—which can be ignored for coupled gas or solid-state lasers—is the delay of the mutually injected signal. As we shall demonstrate numerically, the delay is responsible for a different form of quasiperiodic synchronization. The laser oscillations are now characterized by the frequency f_1 (or f_2) and a frequency proportional to the inverse delay time τ. Furthermore, the intensities of the two lasers may oscillate with different amplitudes. This localized quasiperiodic regime may appear as a secondary bifurcation from a stable localized periodic state and has a better chance to be observed than the mixed-mode quasiperiodic synchronization. Because distinct mechanisms may lead to periodic or quasiperiodic synchronization, it will be useful to have a simple analytical understanding of the laser bifurcations. To this end, we take advantage of the natural values of the laser parameters and formulate simplified nonlinear equations which we then analyze by using perturbation methods. The analysis only considers the case of zero delay. We investigate the effect of the delay by studying numerically the bifurcation diagram of the original laser rate equations. Two by-products of our combined analytical and numerical study are as follows. First, we note that the lasers need to be nonidentical in order to observe synchronization. Second, we show that the branch of localized periodic states may unfold near a secondary bifurcation otherwise known in the mathematical literature as imperfect pitchfork bifurcation [13] and exhibit multiple periodic attractors.

The paper is organized as follows. In Sec. II we describe our experimental setup of two mutually coupled semiconductor lasers and briefly report on the observation of localized synchronization which motivates our new analysis of the laser equations. We introduce the model for the two mutually coupled semiconductor lasers which is based on single mode rate equations in Sec. III. Numerical computations are presented showing that these equations describe the experimental findings. In Sec. IV we predict other synchronization mechanisms by analyzing a reduced phase model of two mutually coupled semiconductor lasers. We perform a bifurcation analysis of the periodic states and analyze their stability properties. Further numerical computations are described in Sec. V in order to clarify the role of the delay. In Sec. VI our results are summarized, and we compare and contrast our findings with other interesting issues of coupled semiconductor lasers, such as two coupled identical lasers, operation close to threshold, and evanescently versus mutually coupled.

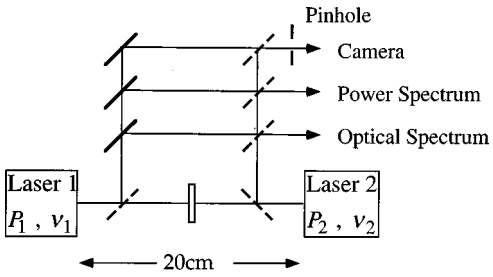

FIG. 1. Our experimental setup consists of two commercially available Sharp LT015 lasers emitting at 830 nm. They are placed at a distance of $L=20$ cm. Two collimating lenses were used to mode-match the beams of the two lasers. The coupling strength was controlled by a set of three polarizers. Symmetric mutual coupling was ensured by imaging the beam of the lasers. The optical spectrum was measured with a scanning Fabry-Pérot interferometer with a free spectral range of 2000 GHz. The radio frequency spectrum was monitored with a HP8596E.

II. EXPERIMENTAL SETUP AND OPTICAL SPECTRA

Our intent is to study the temporal characteristics of an array of evanescently coupled semiconductor lasers as a function of coupling strength. However, systematic experiments on coupled semiconductor laser arrays are very difficult to realize because such a device allows very little control of its operating parameters. One would have to fabricate a new device for each value of coupling strength while keeping all other laser parameters identical. This is naturally a very time consuming and expensive procedure. Another difficulty is to decouple pump currents of the individual lasing elements while maintaining sufficient optical coupling. We therefore chose two commercially available semiconductor lasers and mutually coupled them by injecting light from one into the other. This configuration allowed us to independently control the coupling strength, the detuning between the optical frequencies of the lasers, and their individual pump levels. It also permitted us to study the effect of coupling two distinctly nonidentical lasers. We deliberately kept the coupling strength weak in order to avoid the excitation of more than one external cavity mode [14]. We extracted the underlying dynamics by observing the optical spectra since experiments using streak cameras [3] and theoretical computations [4] have shown that intensity fluctuations in coupled semiconductor lasers typically take place at a subnanosecond time scale, which renders direct observations of long and high-quality time traces very difficult.

In the experiment we used two commercially available single-mode semiconductor lasers (Sharp LT015 lasing at 830 nm) and coupled them at a distance of $L=20$ cm. Two collimating lenses were used to mode-match the beams of the two lasers. The coupling strength was controlled by a set of three polarizers so that less than 10^{-4} of the intensity of one laser was injected into the other (Fig. 1). Symmetric

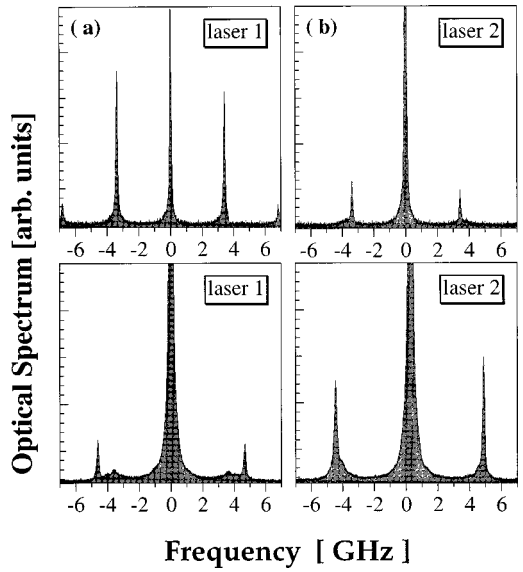

FIG. 2. Experimental optical spectra of the two lasers demonstrating localized synchronization. Less than 10^{-4} of the intensity of one laser is injected into the other and for zero optical detuning we see strong undamped relaxation oscillation sidebands at f_1 (a). Laser 2 also exhibits sidebands at f_1, but the oscillation strength is much weaker (b). As we detune laser 2 from laser 1 resonantly by $\nu_1-\nu_2=f_2$, we find that laser 2 exhibits strong relaxation oscillation sidebands at f_2 (d) and laser 1 is entrained to f_2; however, the oscillation strength is weaker (c).

mutual coupling was ensured by imaging the beam of laser 1 and the light of laser 2, which passed the polarizers and was reflected from the front facet of laser 1, through a pin hole on the same spot. The same procedure was repeated for the beam of laser 2 and the transmitted beam of laser 1 to verify the alignment. Through adjustments of the temperature, the lasers were tuned to the same optical frequency (i.e., $\nu_1=\nu_2$), but their pump levels were kept dissimilar. Laser 1 was pumped at 47% and laser 2 at 55% above threshold, resulting in output powers of 24.4 and 33.4 mW, and free-running relaxation oscillation frequencies of $f_1=3.77\pm0.05$ GHz and $f_2=4.43\pm0.05$ GHz, respectively. The optical spectrum was monitored with a scanning Fabry-Pérot interferometer which had a free spectral range of 2000 GHz (Newport SR-240C). The absence of beat frequencies in the radio frequency spectrum (HP 8596E) verified that each of the lasers was lasing at only one single external cavity mode.

Figures 2(a) and 2(b) show the optical spectra of laser 1 and laser 2 with weak coupling. The relaxation oscillation frequency f_1 of laser 1 is undamped as indicated by strong relaxation oscillation sidebands at f_1 [Fig. 2(a)]. The spectrum of laser 2 [Fig. 2(b)] recorded for the same coupling strength shows sidebands that are also located at f_1 but that are considerably weaker. Thus the two coupled lasers exhibit a form of localized synchronization characterized by frequency f_1. Note that laser 2 is pumped at a high level but is forced to oscillate at the relaxation oscillation frequency of laser 1 which is pumped at a lower level. As we further increase the mutual coupling strength, we find that external cavity modes are excited and the laser output becomes quasiperiodic.

A successful synchronization between lasers can be modified if we resonantly detune the two lasers. Specifically, we have also observed that laser 1 may be entrained to laser 2 at frequency f_2 as we resonantly detune laser 1 from laser 2 by $\nu_1-\nu_2=f_2$. Figures 2(c) and 2(d) show the optical spectra for each laser, respectively. We see that laser 2 exhibits strong relaxation oscillation sidebands at the relaxation oscillation frequency f_2 and laser 1 is entrained to the same frequency with a weaker oscillation strength. In this paper, we concentrate on possible synchronization mechanisms resulting from coupling only and do not consider these cases of resonance.

III. LASER RATE EQUATIONS AND NUMERICALLY COMPUTED SPECTRA

The system of these two mutually coupled semiconductor lasers can be modeled using single-mode rate equations. Each laser is described by one equation for the normalized complex electric field, E_m $(m=1,2)$, and one for the normalized carrier number above threshold, N_m [8]. The coupling is accounted for by adding a delayed electric field of laser 2, $E_2(t-\tau)$, with a real coupling efficiency of η_1 to the equation for the complex electric field of laser 1 and vice versa [15]. Self-coupling caused by reflections from the front facet of one laser back into the other is neglected because it is of $O(\eta_m^2)$ small and is therefore much smaller than the cross-coupling [16]. The complete set of equations in dimensionless form is given by

$$E_1'=(1+i\alpha)N_1E_1+\eta_1E_2(t-\tau)+i\omega_1E_1, \tag{1}$$

$$E_2'=(1+i\alpha)N_2E_2+\eta_2E_1(t-\tau)+i\omega_2E_2, \tag{2}$$

$$TN_1'=P_1-N_1-(1+2N_1)|E_1|^2, \tag{3}$$

$$TN_2'=P_2-N_2-(1+2N_2)|E_2|^2. \tag{4}$$

Primes indicate derivatives with respect to time t, where time is measured in units of the photon lifetime τ_p, α is the linewidth enhancement factor, $\omega_m\equiv2\pi\tau_p\nu_m$ denotes the normalized optical frequencies of each laser which we assume equal. T is the ratio of the carrier lifetime τ_s to τ_p. The delay time $\tau\equiv L/c\tau_p$ corresponds to the time it takes for the light to travel the distance L from one laser to the other. P_m denotes the pumping above threshold for each laser. This dynamical system shares common features with the well-studied injection model [17], delayed feedback model [18], and the system of two evanescently coupled semiconductor lasers [19]. We therefore anticipate that our system of two mutually coupled lasers exhibits similarities to all these models.

We numerically integrated Eqs. (1)–(4) using typical parameters for the sharp LT015 diode lasers used in the experiment: $\tau_p=1.4$ ps, $\tau_s=1$ ns $(T=714)$, $L=20$ cm $(\tau=476)$, $\alpha=5$, $\omega_1=\omega_2$, and $\omega_m\tau=2n\pi$, n integer. The lasers were pumped at $P_1=0.402$ and $P_2=0.555$ above threshold to approximately match the free-running relaxation frequencies of f_1 and f_2 in the experiment. Figure 3 displays optical spectra for various values of coupling strength η_1 keeping the ratio

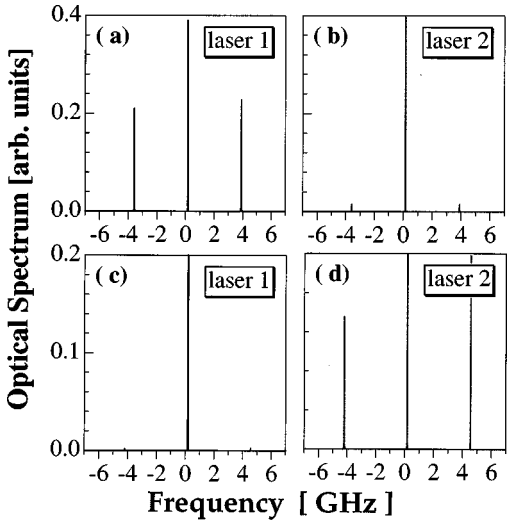

FIG. 3. Optical spectra computed from Eqs. (1)–(4) for $\tau_p = 1.4$ ps, $\tau_s = 1$ ns ($T \simeq 714$), $L = 20$ cm ($\tau = 476$), $\alpha = 5$, $P_1 = 0.402$, $P_2 = 0.555$, $\omega_m \tau = 2n\tau$, $C = 1$, and $n_1 = 10^{-3}$. Laser 1 shows strong sidebands at f_1 (a) and laser 2 shows weak sidebands also at f_1 (b) demonstrating localized synchronization. The two lasers can be entrained at the relaxation oscillation frequency of laser, f_2, for $C = 2$ and $n_1 = 6.1 \times 10^{-4}$. The optical spectrum of laser 1 shows weak relaxation oscillation sidebands at f_2 (c). The optical spectrum of laser 2 shows strong relaxation oscillation sidebands at f_2 (d).

$$C \equiv \eta_2 / \eta_1 \tag{5}$$

equal to 1. For a coupling strength of $\eta_1 = 1.0 \times 10^{-3}$ [Fig. 3(a)], laser 1 exhibits strong undamped relaxation oscillation sidebands at f_1 and laser 2 [Fig. 3(b)] has sidebands at f_1 as well but smaller in amplitude. Thus, laser 2, which is pumped at a higher level, is entrained to the relaxation oscillation frequency of laser 1. Since the intensity oscillations of laser 1 are much larger than the intensity oscillations of laser 2, the synchronization is localized. As the coupling strength is increased, external cavity modes are excited and the laser output becomes quasiperiodic. In our numerical calculations we can change the ratio of the two coupling strengths C and examine its effects. We find that for $C > P_2/P_1 \simeq 1.38$, the relaxation oscillation frequency of laser 2, namely f_2, is strongly undamped and laser 1 is entrained to laser 2 at frequency f_2. In this case the oscillation strength of laser 1 is significantly weaker than that of laser 2 and synchronization is again localized. The optical spectra are depicted in Figs. 3(c) and 3(d) for $C = 2$ and $\eta_1 = 6.1 \times 10^{-4}$. We also investigated the bifurcation diagram of the solutions of Eqs. (1)–(4) using the same values of the parameters as in Figs. 3(a) and 3(b). These results are summarized in the numerical section below. The two coupled lasers undergo a bifurcation from steady to time-periodic intensities. The frequency of the oscillations is f_1 and the amplitude of the oscillations of laser 2 is much smaller than the amplitude of the oscillations of laser 1.

In summary, we have observed experimentally and numerically that the two mutually coupled semiconductor lasers can exhibit localized synchronization (i.e., single-mode operation) which is the simplest form of interaction between the lasers. We also found numerically that the localized state depends on the value of the asymmetric coupling factor C and that quasiperiodic forms of synchronization may appear as we increase the coupling strength. In order to identify the mechanisms leading to these quasiperiodic synchronizations, we propose a bifurcation analysis in the next section.

IV. REDUCED LASER EQUATIONS AND BIFURCATION ANALYSIS

Specifically, we reduce Eqs. (1)–(4) to a simpler and analytically tractable form by taking advantage of the two large parameters that are inherently present in semiconductor lasers, the ratio T of the two fundamental time scales, τ_p and τ_s, and the linewidth enhancement factor α. We have verified numerically that the solution of the reduced problem is in good agreement with the solution of the full laser equations (1)–(4) if $T = 1000$ and $\alpha = 10$. For smaller values of $\alpha (\alpha \geqslant 5)$, we have found that the bifurcation diagrams of the full and reduced laser equations remain in semiquantitative agreement (i.e., same bifurcation transitions and same orders of magnitude of the various solutions).

The asymptotic method leading to the simplified laser problem is similar to the method used in [20–22] for different laser problems. After substituting the new time

$$s \equiv \Omega t \tag{6}$$

into Eqs. (1)–(4), where

$$\Omega \equiv \sqrt{2P_1/T} \ll 1 \tag{7}$$

is the relaxation oscillation frequency of laser 1, we introduce the new variables e_m, Ψ_m, and n_m defined by

$$\begin{aligned} E_m &= \sqrt{P_m}(1 + e_m/\alpha)\exp[i(\Psi_m + \omega_m t)], \\ N_m &= \Omega n_m / \alpha, \end{aligned} \tag{8}$$

and neglect all $O(1/\alpha)$ correction terms. The resulting equations can be reformulated in terms of Ψ_1 and Ψ_2 only and are given by the following two coupled third-order delay-differential equations:

$$\Psi_1''' + \xi_1 \Psi_1'' + \Psi_1' = -r\Lambda_1 \cos[\psi_1(s)], \tag{9}$$

$$\Psi_2''' + \xi_2 \Psi_2'' + r^2 \Psi_2' = -r\Lambda_2 \cos[\psi_2(s)], \tag{10}$$

where primes means differentiation with respect to time s. In these equations, ψ_1 and ψ_2 are the coupling functions defined by

$$\psi_1(s) \equiv \Psi_2(s - \Omega\tau) - \Psi_1(s) - \omega_2 \tau - \Delta s, \tag{11}$$

$$\psi_2(s) \equiv \Psi_1(s - \Omega\tau) - \Psi_2(s) - \omega_1 \tau + \Delta s, \tag{12}$$

where

$$\Delta \equiv (\omega_1 - \omega_2)/\Omega \tag{13}$$

is the scaled detuning between the optical frequencies. The parameters Λ_m, ξ_m, and r are defined by

$$\Lambda_m \equiv \alpha \eta_m / \Omega, \quad \xi_m \equiv (1+2P_m)/\Omega T, \qquad r \equiv \sqrt{P_2/P_1}. \tag{14}$$

Λ_m is proportional to the mutual coupling strength, ξ_m is the damping constant, and r^2 is the ratio of the two pumps.

Physically, these phase equations describe two oscillators, one oscillating with frequency $\sigma_1=1$ and the other with frequency $\sigma_2=r$ ($\sigma_m \equiv 2\pi f_m \tau_p/\Omega$). Both oscillators are driven nonlinearly by the $\cos(\psi_m)$ term. Equations (9) and (10) have a simple interpretation when the delay τ is neglected. Then the system further reduces to two phase oscillators, which are driven nonlinearly by their common phase difference, $\cos(\Psi_1-\Psi_2)$.

In order to determine an analytical solution of Eqs. (9) and (10), we shall consider the case of weak coupling ($\Lambda_m \ll 1$) and zero delay. However, a nonzero delay is not a limitation of our analysis. The delay is responsible for quasiperiodic instabilities that we shall describe in the next section. We also consider the case $\omega=\omega_1=\omega_2$ ($\Delta=0$). The details of the analysis are long and tedious (see [23]) and we summarize the main results. The leading-order approximation of the coupled phase equations (9) and (10) is given by

$$\Psi_1 \simeq A_1 \sin(s+\phi_1)+B_1, \tag{15}$$

$$\Psi_2 \simeq A_2 \sin(rs+\phi_2)+B_2, \tag{16}$$

where A_m, B_m, and ϕ_m are slowly varying functions of time s. They satisfy amplitude equations which are determined by applying solvability conditions. The slow time equations for A_1, A_2, and $\Theta \equiv B_2-B_1$ are given by

$$A_1' = -\tfrac{1}{2}\xi_1 A_1 + r\Lambda_1 \sin(\Theta) J_0(A_2) J_1(A_1), \tag{17}$$

$$A_2' = -\tfrac{1}{2}\xi_2 A_2 - \frac{\Lambda_2}{r}\sin(\Theta) J_0(A_1) J_1(A_2), \tag{18}$$

$$\Theta' = -F\cos(\Theta) J_0(A_1) J_0(A_2), \tag{19}$$

where F is defined by

$$F \equiv \frac{\Lambda_2}{r} - r\Lambda_1. \tag{20}$$

In these equations, $J_0(A_m)$ and $J_1(A_m)$ denote Bessel functions of A_1 or A_2. Equations (17)–(19) are our bifurcation equations that we propose to analyze. Recall that $C \equiv \eta_2/\eta_1 = \Lambda_2/\Lambda_1$ is defined as the ratio of the coupling strengths. Our analysis of the primary solutions of Eqs. (17)–(19) shows that there exist two cases depending on the value of C. If

$$C < C^\star \equiv r^2 = \frac{P_2}{P_1}, \tag{21}$$

we find that the first bifurcation of the basic state $(A_1,A_2)=(0,0)$ is a bifurcation to a pure mode solution $(A_1,A_2)=(A_1,0)$, where $A_1(\Lambda_1)$ satisfies the implicit equation $\Lambda_1 = \xi_1 A_1/2rJ_1(A_1) > 0$. This bifurcation occurs at

$$\Lambda_1^{H1} \equiv \frac{\xi_1}{r} = \frac{1+2P_1}{\Omega T}\left(\frac{P_1}{P_2}\right)^{1/2} \tag{22}$$

and corresponds to a Hopf bifurcation of the original laser equations since A_1 multiplies $\sin(s+\phi_1)$ in expression (15). After the bifurcation, the oscillations of $\Psi_1(s)$ are $O(1)$ in amplitude and exhibit a frequency $\sigma_1=1$. The oscillations of $\Psi_2(s)$ admit the same frequency but are $O(\Lambda_2)$ small, as shown by the higher-order correction of the perturbation solution.

On the other hand, if

$$C > C^\star, \tag{23}$$

we observe an analogous bifurcation scenario, only that laser 1 is now entrained to laser 2 at $\sigma_2=r$. The first primary bifurcation is now leading to the pure mode solution $(A_1,A_2)=(0,A_2)$ and is located at

$$\Lambda_1^{H2} = C^{-1}\xi_2 r = C^{-1}\frac{1+2P_2}{\Omega T}\left(\frac{P_2}{P_1}\right)^{1/2}. \tag{24}$$

The determination of the primary bifurcation points (22) and (24) is important because they allow us to explain our observations of localized synchronization. The critical point $C=C^*$ verifies the condition $F=0$, where F is defined by Eq. (20). It corresponds to a change of stability of the phase Θ and does not mean $\Lambda_1^{H2}=\Lambda_1^{H1}$ [note: Λ_1^{H2} and Λ_1^{H1} are bifurcation points from two distinct steady states: $(A_1,A_2,\Theta)=(0,0,\pi/2)$ and $(A_1,A_2,\Theta)=(0,0-\pi/2)$, respectively].

As Λ_1 is progressively increased from zero, secondary bifurcations appear. We only describe the case (21) for clarity. The bifurcation diagram of the steady-state amplitudes A_1 and A_2 is shown in Fig. 4. The pure mode solution that emerges at $\Lambda_1=\Lambda_1^{H1}$ is characterized by a constant $\Theta=\pi/2$ and is stable provided that $J_0(A_1)>0$. At $A_1=A^*$, where $A^*\simeq 2.4$ is defined as the first zero of $J_0(A_1)$, the pure mode solution $A_1\neq 0$, $A_2=0$ undergoes a secondary bifurcation to another pure mode solution characterized by $A_1=A^*$ remaining constant but now Θ being a function of Λ_1. This new solution corresponds to a new periodic state of the original laser equations. The secondary bifurcation is located at $\Lambda_1=\Lambda_1^{*1}$ in Fig. 4. The bifurcation is a pitchfork bifurcation with two distinct branches $\Theta=\Theta(\Lambda_1)$ for $\Lambda_1 \geqslant \Lambda_1^{*1}$. In addition to the cascading bifurcations following $\Lambda_1=\Lambda_1^{H1}$, we observe a second primary bifurcation from $(A_1,A_2)=(0,0)$ to the pure mode $A_1=0$, $A_2\neq 0$ which appears at $\Lambda_1^{H2}>\Lambda_1^{H1}$. However, this solution is unstable near Λ_1^{H2} and stabilizes only as A_2 surpasses $A^*\simeq 2.4$. This secondary bifurcation is located at $\Lambda_1=\Lambda_1^{*2}$ in Fig. 4. Then, a stable pure mode periodic state exhibiting frequency $\sigma=r$ may coexist with one of the periodic solution that follows the branching at $\Lambda_1=\Lambda_1^{H1}$. Finally, this stable periodic solution $A_1=0$, $A_2\neq 0$ changes stability at $\Lambda_1=\Lambda_1^M$ and leads to a mixed-mode solution characterized by the two relaxation oscillation frequencies and comparable amplitudes.

Other branches of periodic states are possible because the Bessel functions appearing in our bifurcation equations are

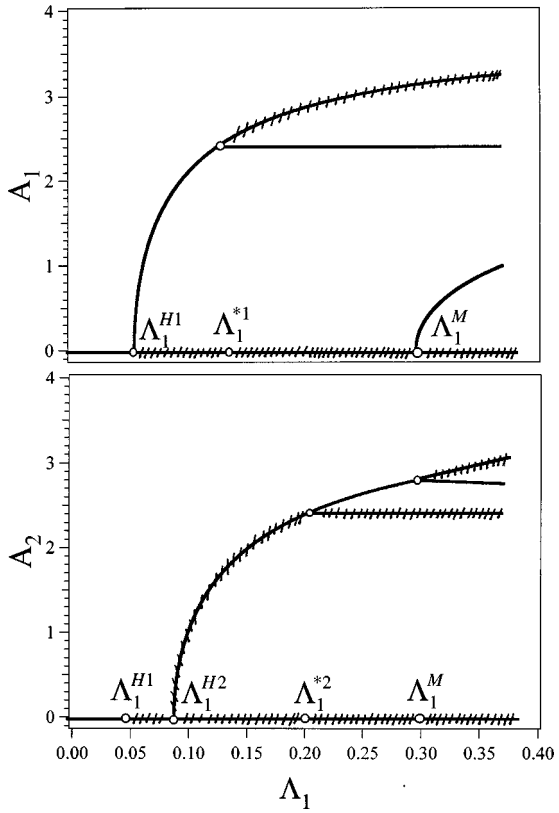

FIG. 4. Bifurcation diagram of the steady-state amplitudes A_1 and A_2. The different solutions are obtained analytically from Eqs. (17)–(19). The figures exhibit two distinct primary bifurcations to single-mode solutions located at Λ_1^{H1} and Λ_1^{H2}, respectively. Because $\Lambda_1^{H1}<\Lambda_1^{H2}$, the two lasers synchronize into a localized state with frequency f_1 as Λ_1 surpasses Λ_1^{H1}. The points denoted by Λ_1^{*1} and Λ_1^{*2} are two distinct secondary bifurcations which appear at $A_1=A^*$ and $A_2=A^*$, respectively. Λ_1^{*1} corresponds to a bifurcation from one stable periodic state to another stable periodic state. Λ_1^{*2} marks the change of stability of the pure mode solution $(A_1,A_2)=(0,A_2)$. As $\Lambda_1>\Lambda_1^{*2}$, the two pure mode solutions coexist in the bifurcation diagram. At $\Lambda_1=\Lambda_1^M$, we observe the bifurcation to a mixed-mode solution characterized by nonzero values of both A_1 and A_2. This solution corresponds to a quasiperiodic regime of the laser rate equations.

multivalued functions. These branches of solutions appear for larger values of Λ_1 and are not shown in Fig. 4.

In summary, the bifurcation analysis revealed that in addition to the two primary bifurcations (i.e., $\Lambda_1=\Lambda_1^{H1}$ and $\Lambda_1=\Lambda_1^{H2}$), the coupled lasers admit a bifurcation to a new periodic state ($\Lambda_1=\Lambda_1^{*1}$), a bifurcation which allows the coexistence of periodic states exhibiting different frequencies ($\Lambda_1=\Lambda_1^{*2}$), and a bifurcation to a quasiperiodic mixed modes regime ($\Lambda_1=\Lambda_1^M$). The latter is an interesting new form of synchronization because the intensities of the two lasers are comparable and because they exhibit two relaxation oscillation frequencies.

We have verified the results of our analysis based on the limit Λ_1 small by integrating numerically Eqs. (9) and (10) for $T=1000$, $\alpha=10$, and $\tau=0$. See Fig. 5. We have found all our stable solutions and the numerical bifurcation points in Fig. 5 are in excellent agreement with their analytical estimates shown in Fig. 4. In the next section, we study the full

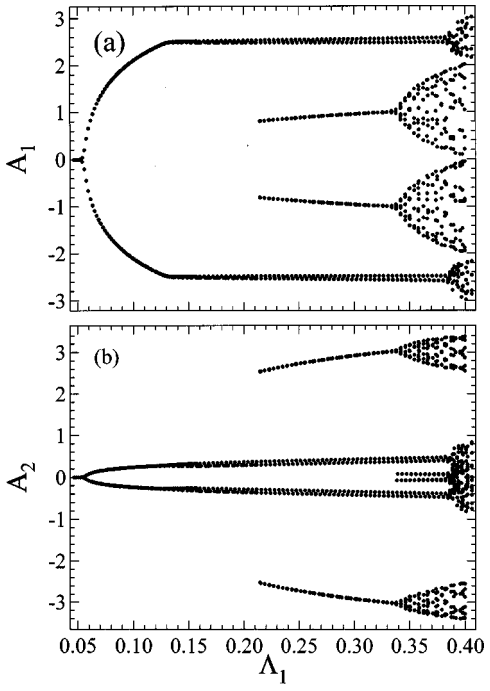

FIG. 5. Numerical bifurcation diagram of the two coupled phase equations (9) and (10). The figures represent the deviations of the maxima and minima of the two intensities from their steady-state values. The diagram exhibits all the stable periodic and quasiperiodic solutions. For the periodic states, the deviations of the intensities are well approximated by the amplitudes $\pm A_1$ and $\pm A_2$, respectively. Note that the branches of solutions have been determined by either increasing or decreasing continuously the control parameter and by starting with different initial conditions when stable branches overlap.

laser equations (1)–(4) with particular attention to (i) the periodic solutions near the secondary bifurcation at $\Lambda_1=\Lambda_1^{*1}$ and (ii) a new quasiperiodic instability caused by the delay.

V. NUMERICAL STUDY OF THE LASER RATE EQUATIONS

The objective of our numerical study is twofold. We first wish to examine the secondary bifurcation to the new periodic state which is suggested by our analysis and which appears as amplitude A_1 surpasses $A^*\simeq 2.4$. Second, we concentrate on the possible bifurcations to quasiperiodic regimes.

In the first case, we note numerically that the secondary bifurcation is unfolded. Specifically, a pitchfork secondary bifurcation at $\Lambda_1=\Lambda_1^{*1}$ becomes asymmetric and leads to a stable and isolated branch of periodic states and to a smooth branch of primary periodic states. This unfolding is not predicted by the analysis of the amplitude equations (17)–(19) and requires a higher-order analysis near the secondary bifurcation point at $\Lambda_1=\Lambda_1^{*1}$. We have verified analytically that the unfolding is essentially determined by the correction terms multiplying the coupling terms η_1 and η_2. An immediate consequence of this unfolding is that the branch of primary states does not exhibit a secondary bifurcation point if the control parameter is slowly increased from zero. We

note that the straight line $A_1=2.4$ in Fig. 4 splits in two lines. The lower line smoothly connects the primary bifurcation point Λ_1^{H1} while the upper line connects the upper unstable branch in Fig. 4 through a limit point located near Λ_1^{*1}.

The bifurcation to the quasiperiodic oscillations is physically more interesting because we numerically find bifurcations that were not predicted by our analysis. These new bifurcations to quasiperiodic oscillations are produced by the relatively large delay which forces the laser system to adopt a two-times response (i.e., the relaxation oscillations time f_1^{-1} and the delay time τ). By decreasing τ, we clearly note that these bifurcations go to larger Λ_1 but that the branch of mixed-mode quasiperiodic oscillations predicted by our analysis only slightly changes.

Figure 6 is a representative bifurcation diagram that displays both the results of the unfolding of the secondary bifurcation and three bifurcations to quasiperiodic oscillations. Figure 7 shows the bifurcation diagram of the laser rate equations using the values of the parameters given in Fig. 3 and which best simulate our experiments.

VI. SUMMARY AND DISCUSSION

We have shown that two mutually coupled semiconductor lasers exhibiting different values of the parameters may synchronize in different ways. The simple synchronization mechanism is a single-mode form of synchronization where one laser is forced to oscillate at the relaxation oscillation frequency of the other laser and with relatively smaller amplitude. It has been called localized synchronization and it has been observed experimentally. However, richer synchronization patterns are possible which exhibit two distinct frequencies. We have found a quasiperiodic regime characterized by the two individual laser relaxation oscillations frequencies and a quasiperiodic regime where one frequency corresponds to a relaxation oscillation frequency of one of the two individual lasers and one frequency proportional to the inverse delay time. Although these two forms of quasiperiodic entrainment can be stable, only the second regime is expected to be seen if we gradually increase the injection rate from zero, as suggested by Fig. 7. The first regime is isolated in the bifurcation diagram and cannot be reached using a continuation method. On the other hand, the second quasiperiodic regime appears from a bifurcation of the primary localized state and will be localized too. Experimentally, we have found evidence of quasiperiodic synchronization at relatively high injection rates but frequencies are harder to identify due to the possible presence of multiple external cavity modes.

We next review a series of problems that are directly related to our analysis. The question arises whether two semiconductor lasers having the same values of the parameters can exhibit synchronization as they are mutually coupled. We have investigated this system [Eqs. (1)–(4)] numerically for zero optical frequency detuning, symmetric coupling strength, and identical pump levels. The parameter values were $\tau_p=1.43$ ps, $\tau_s=1$ ns ($T\simeq 700$), $P_1=P_2=0.402$, $\alpha=5$, $C=1$, $\omega_1=\omega_2$, and $\omega_m\tau=2n\pi$, n integer. As we included the delay, we found that there are three stable states: one for which both lasers oscillate in synchrony with identical amplitudes, and two localized states for which either laser

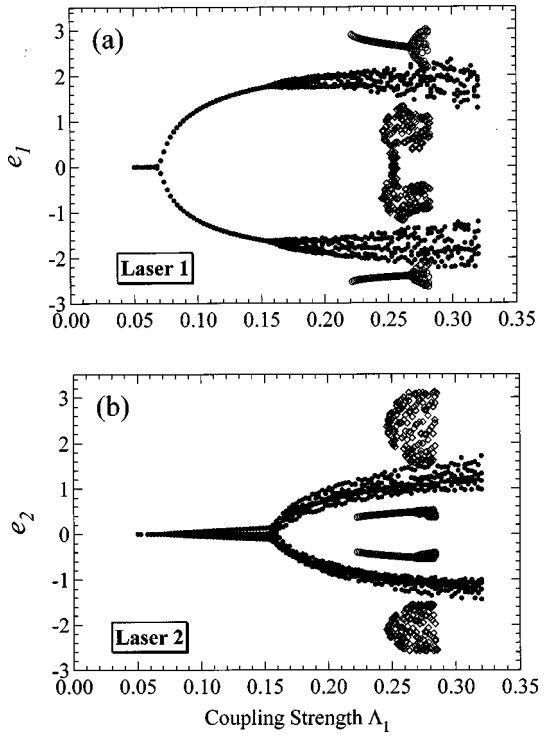

FIG. 6. Numerical bifurcation diagram of the laser rate equations (1)–(4). The figures represent the deviations of the maxima and minima of the two intensities from their steady-state values [e_1 and e_2 are defined by Eq. (8)]. The diagram exhibits all the stable periodic and quasiperiodic solutions. The values of the parameters are $C=1$, $P_1=0.402$, $P_2=0.555$, $T=2000$, $\alpha=6$, and $\tau=476$. The figures show a primary bifurcation to a pure mode periodic solution ($A_1\neq 0$, $A_2=0$). It emerges from a Hopf bifurcation located at $\Lambda_1\simeq 0.07$, and it is designated with bullets (●). Near the critical amplitude $A_1=A^*\simeq 2.4$, the unfolding of the pitchfork secondary bifurcation leads to an isolated branch of periodic states that is designated with circles (○). Both branches (bullets and circles) undergo bifurcation to quasiperiodic oscillations which are caused by the relatively large delay τ (frequencies close to f_1 and τ^{-1}). These bifurcations move to infinity if τ is decreased. The figures also show the branch of mixed-mode quasiperiodic oscillations (frequencies f_1 and f_2). The branch is shown by diamonds (◇). This branch is stable after a second, secondary bifurcation of the pure mode periodic solution ($A_1=0$, $A_2\neq 0$). We also found a small domain where this solution is stable before the quasiperiodic oscillations. Note that the secondary bifurcation to quasiperiodic oscillations near $\Lambda_1=0.15$ is the first instability that appears after the primary bifurcation point at $\Lambda_1\simeq 0.07$.

1 is the strong oscillator and laser 2 is the weak one or vice versa. We varied the delay from $\tau=476$ to $\tau=10$ and observed that the Hopf bifurcation point moved to larger values of the coupling strength suggesting that this bifurcation is controlled by τ. Yet for the simplest case of zero delay the system stays in steady state and does not exhibit instabilities.

Another interesting question is whether synchronization can be observed as one of the lasers is pumped close to its lasing threshold. Our numerical calculations for zero delay in Eqs. (1)–(4) show that as laser 2 is pumped slightly above threshold the same scenario of localization takes place as in the case of both pumps above threshold. The parameter values were $\tau_p=1.43$ ps, $\tau_s=1$ ns ($T\simeq 700$), $\tau=0$, $P_1=0.3$, $P_2=0.005$, $\alpha=5$, $C=1$, $\omega_1=\omega_2$, and $\omega_m\tau=2n\pi$, n inte-

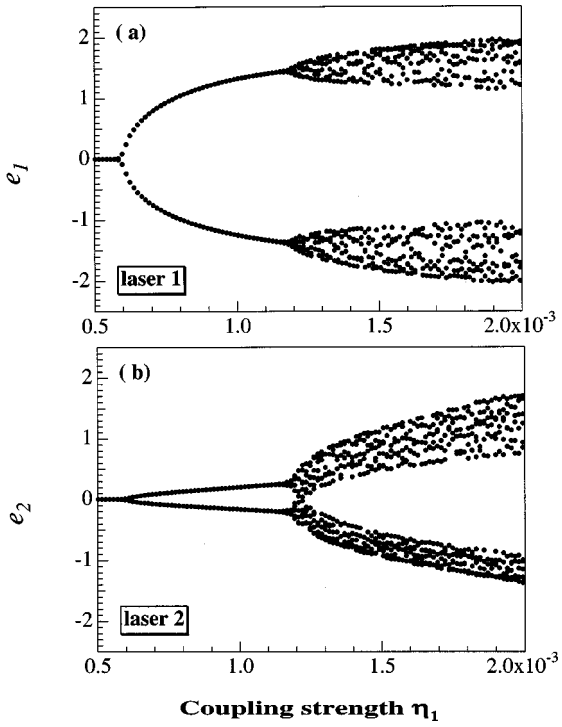

FIG. 7. Numerical bifurcation diagram of the laser rate equations (1)–(4). The figures represent the deviations of the maxima and minima of the two intensities from their steady-state values as a function of η_1. The values of the parameters are the same as in Fig. 3. We note that the primary bifurcation to the localized state is quickly followed by a bifurcation to quasiperiodic oscillations and is caused by the delay.

ger. We find that again the weakly pumped laser 2 is destabilized, undergoes a Hopf bifurcation, and the strongly pumped laser 1 entrains to the relaxation oscillation frequency f_2 of laser 2. However, the modulation depth of laser 1 is very small. As laser 2 is pumped below threshold ($P_2 = -0.005$), the reverse scenario takes place, meaning the strongly pumped laser 1 is destabilized for rather strong coupling and the weakly pumped laser 2 entrains to the relaxation oscillation frequency f_1 of laser 1.

Finally it is important to know whether localized synchronization can be found in two evanescently coupled semiconductor lasers [19] as well. We have studied numerically the coupled-mode model considered in [19] using the same parameter values as for Fig. 3 and setting the delay to zero. In the weak coupling regime the two lasers bifurcate from steady state into a limit cycle for $\Lambda = 0.065$, which is very close to the theoretically predicted Hopf point in the case of two mutually coupled lasers. In addition, the oscillatory synchronization between the lasers is clearly localized suggesting that the phenomenon of localized synchronization is quite general as soon as the two lasers exhibit different parameter values. However, if the two lasers have identical parameters, Hopf bifurcations are no more possible for two mutually coupled lasers (no delay) while they still exist for two evanescently coupled lasers. This is a consequence of the coupling mechanism being real for the mutually coupled lasers while being imaginary for the evanescently coupled lasers.

ACKNOWLEDGMENTS

A.H. wishes to thank the NRC and the AFOSR for supporting her work. T.E. was supported by U.S. AFOSR Grant No. AFOSR F49620-95-0065, NSF Grant No. DMS-9625843, NATO Grant No. 961113, the Fonds National de la Recherche Scientifique (Belgium), and the InterUniversity Attraction Pole of the Belgian Government. V.K. was supported by the AFOSR through a University Research Resident Program.

[1] D. R. Scifres, R. D. Burnham, and W. Streifer, Appl. Phys. Lett. **33**, 1015 (1978).
[2] N. W. Carlson, *Monolithic Diode-Laser Arrays* (Springer-Verlag, New York, 1994); D. Botez and D. R. Scifres, *Diode Laser Arrays* (Cambridge University Press, New York, 1994).
[3] R. A. Elliott, R. K. DeFreez, T. L. Paoli, R. D. Burnham, and W. Streifer, IEEE J. Quantum Electron. **21**, 598 (1985).
[4] S. S. Wang and H. G. Winful, Appl. Phys. Lett. **52**, 1774 (1988).
[5] J. D. Murray, *Mathematical Biology* (Springer-Verlag, Berlin, 1989).
[6] D. G. Aronson, G. B. Ermentrout, and N. Kopell, Physica D **41**, 403 (1990).
[7] R. Kuske and T. Erneux, Opt. Commun. **139**, 125 (1997).
[8] H. G. Winful and L. Rahman, Phys. Rev. Lett. **65**, 1575 (1990); H. G. Winful, in *Nonlinear Dynamics and Spatial Complexity in Optical Systems*, edited by R. G. Harrison and J. S. Uppal, Scottish University Summer School in Physics, 1993 (Institute of Physics, Bristol, 1992), p. 217.
[9] R. Roy and K. S. Thornburg, Phys. Rev. Lett. **72**, 2009 (1994).
[10] K. S. Thornburg, M. Möller, R. Roy, T. W. Carr, R.-D. Li, and T. Erneux, Phys. Rev. E **55**, 3865 (1997).
[11] K. S. Thornburg (private communication).
[12] A. Hohl, A. Gavrielides, T. Erneux, and V. Kovanis, Phys. Rev. Lett. **78**, 4745 (1997).
[13] G. Iooss and D. D. Joseph, *Elementary Stability and Bifurcation Theory* (Springer-Verlag, New York, 1980), p. 32.
[14] G. C. Dente, C. E. Moeller, and P. S. Durkin, IEEE J. Quantum Electron. **26**, 1014 (1990).
[15] D. J. Bossert, R. K. DeFreez, G. C. Dente, and H. G. Winful, in *Nonlinear Dynamics in Optical Systems Technical Digest, 1992* (Optical Society of America, Washington, D.C., 1992), Vol. 16, p. 272.
[16] We have experimentally tested whether self-coupling affects the laser dynamics. As we set the polarizers to the coupling strength used in the experiment, we turned off one of the lasers and observed the optical spectrum of the other laser. We did not find any spectral differences compared to the laser spectrum without coupling.
[17] R. Lang, IEEE J. Quantum Electron. **18**, 976 (1982).
[18] R. Lang and K. Kobayashi, IEEE J. Quantum Electron. **16**, 347 (1980).

[19] H. G. Winful and S. S. Wang, Appl. Phys. Lett. **53**, 1894 (1988).
[20] T. Erneux, V. Kovanis, A. Gavrielides, and P. M. Alsing, Phys. Rev. A **53**, 4372 (1996).
[21] T. Erneux, R. Kuske, and T. W. Carr, Proc. SPIE **2792**, 54 (1995).
[22] P. M. Alsing, V. Kovanis, A. Gavrielides, and T. Erneux, Phys. Rev. A **53**, 4429 (1996).
[23] A. Hohl, A. Gavrielides, T. Erneux, and V. Kovanis, Proc. SPIE **2994**, 647 (1997).